Dyes and Pigments 99 (2013) 636–641

Contents lists available at SciVerse ScienceDirect

Dyes and Pigments

journal homepage: www.elsevier.com/locate/dyepig

Novel and environmentally friendly (Bi,Ca,Zn)VO_4 yellow pigments

Toshiyuki Masui, Taihei Honda, Wendusu, Nobuhito Imanaka*

Department of Applied Chemistry, Faculty of Engineering, Osaka University, 2-1 Yamadaoka, Suita, Osaka 565-0871, Japan

ARTICLE INFO

Article history:
Received 4 April 2013
Received in revised form
10 June 2013
Accepted 18 June 2013
Available online 3 July 2013

Keywords:
Bismuth vanadate
Environmentally friendly
Yellow pigment
Solid solution
Monoclinic structure
Liquid phase reaction

ABSTRACT

$Bi_{1-x-y}Ca_xZn_yVO_{4-(x+y)/2}$ ($0 \le x \le 0.10$, $0 \le y \le 0.10$) pigments were synthesized as novel inorganic yellow pigments that are environmentally friendly, and their color properties were characterized. The $Bi_{1-x-y}Ca_x-Zn_yVO_{4-(x+y)/2}$ pigments exhibited brilliant yellow colors, and using the CIE $L^*a^*b^*$ system, the most vivid yellow hue was obtained for $Bi_{0.90}Ca_{0.08}Zn_{0.02}VO_{3.95}$ with a yellowness value (b^*) that is larger than that of a commercially available bismuth vanadate yellow pigment. $BiVO_4$ is an environmentally friendly inorganic yellow pigment, and Ca and Zn are also nontoxic elements; therefore, the $Bi_{0.90}Ca_{0.08}Zn_{0.02}VO_{3.95}$ pigment should be an effective alternative to conventional toxic yellow pigments.

1. Introduction

Inorganic pigments are typically applied to porcelains, ceramic tiles, inks, and paints, due to their high hiding power, weather resistance, and thermal stability. In particular, yellow pigments have a high level of visibility and are employed for road markings. However, several conventional industrial pigments such as chrome yellow ($PbCrO_4$), cadmium yellow (CdS) and cadmium red (CdS/CdSe) contain toxic elements, such as Pb, Cr, Cd, and Se, which have adverse effects on the human body and the environment. Therefore, a number of studies have been reported on new environmentally friendly yellow pigments [1–25]. We have also been working toward the synthesis of several safe yellow pigments to satisfy environmental requirements and the demands of safety-oriented consumers [26–33]. However, there have been no reports of environmentally friendly yellow pigments that exhibit high yellow chromaticity (b^*) in excess of 90 using the CIE $L^*a^*b^*$ system.

In this study, we focused on the improvement of the color of monoclinic bismuth vanadate ($BiVO_4$), which is already known to be an environment-friendly inorganic yellow pigment. The coloring mechanism of monoclinic $BiVO_4$ is based on a charge transfer transition from a hybrid orbital of Bi_{6s} and O_{2p} to V_{3d} in the $BiVO_4$ band structure [34–38]. Replacing some of the Bi or V cations with another one imposes lattice strain or distortion in the lattice, which affects the color of the $BiVO_4$. Actually, it has been reported that bright yellow coloration and enhanced near-infrared reflectance of monoclinic $BiVO_4$ were obtained by the substitution of Ta/P into the vanadium sites of $BiVO_4$ [39].

In this study, on the contrary, we focused on the cation doping at bismuth sites and novel yellow pigments based on monoclinic $Bi_{1-x-y}Ca_xZn_yVO_{4-(x+y)/2}$ ($0 \le x \le 0.10$, $0 \le y \le 0.10$) solid solutions were synthesized in an attempt to find a new environmentally friendly pigment that has sufficient yellow chromaticity. Doping with divalent and smaller Ca^{2+} (ionic radius: 0.112 nm) [40] and/or Zn^{2+} (0.090 nm) [40] into the Bi^{3+} (0.117 nm) [40] sites of the $BiVO_4$ lattice generates intrinsic strain and lattice defects, which alters the O_{2p} valence band and reduces the bandgap energy by modification of the Bi_{6s}/O_{2p} hybrid orbital. Furthermore, both Ca^{2+} and Zn^{2+} are nontoxic elements. Therefore, $Bi_{1-x-y}Ca_xZn_yVO_{4-(x+y)/2}$ pigments were synthesized in this study as new environmentally friendly yellow pigments. The color properties were characterized and the composition was optimized to have the most vivid yellow hue.

2. Experimental

2.1. Materials

The $Bi_{1-x-y}Ca_xZn_yVO_{4-(x+y)/2}$ ($0 \le x \le 0.10$, $0 \le y \le 0.10$) pigments were synthesized using an evaporation to dryness method. A stoichiometric mixture of aqueous solutions of 0.5 mol dm^{-3} $Bi(NO_3)_3$, 0.1 mol dm^{-3} $Ca(NO_3)_2$, and 0.1 mol dm^{-3} $Zn(NO_3)_2$ was added to 30 cm^3 of nitric acid solution (3.0 mol dm^{-3}), in which

* Corresponding author.
E-mail address: imanaka@chem.eng.osaka-u.ac.jp (N. Imanaka).

0143-7208/$ – see front matter © 2013 Elsevier Ltd. All rights reserved.
http://dx.doi.org/10.1016/j.dyepig.2013.06.030

1.08 g of NH_4VO_3 was dissolved. The pH of the mixture was adjusted to 6.5 by dropwise addition of aqueous ammonia (5%). After aging at room temperature for 1 h with stirring, the mixed solution was heated at 453 K until the solvent was vaporized. The resultant solid was calcined at 923 K for 6 h to afford the product.

2.2. Characterization

The pigments were characterized by X-ray powder diffraction (XRD; Rigaku, SmartLab) with Cu Kα radiation (40 kV and 30 mA). The lattice parameters and volumes of the samples were calculated from the XRD peak angles, which were refined using α-Al_2O_3 as a standard, using the CellCalc Ver. 2.20 software. X-ray fluorescence spectroscopy (XRF; Rigaku, ZSX-100e) measurements indicated the sample compositions were in good agreement with the nominal stoichiometric compositions of the starting mixtures. Particle morphology was examined by scanning electron microscopy (SEM; Shimadzu, SS-550). The size distribution and mean particle size were estimated by measuring the diameters of 200 particles from SEM micrographs.

The optical reflectance was measured using a UV–vis spectrometer (Shimadzu, UV-2600) with barium sulfate as a reference. The bandgap energies of the samples were determined from the absorption edge of the absorbance spectra represented by the Kubelka–Munk function, $f(R) = (1 - R)^2/2R$, where R is reflectance [41,42].

The color properties of the green pellets of the prepared samples were estimated in terms of the CIE $L^*a^*b^*$ system using a colorimeter (Konika-Minolta, CR-300). The L^* parameter represents the brightness or darkness of a color relative to a neutral grey scale, while the a^* (the red–green axis) and b^* (the yellow–blue axis) parameters express the color qualitatively.

Raman spectra were obtained with a Jasco NRS-3100 spectrometer using a 532 nm laser as an excitation source, operated at a power of 100 mW, and a CCD detector. Spectra were averaged over 10 scans and recorded at a resolution of 0.1 cm^{-1}. The laser light was directed into an integrated microscope and focused to a spot size of approximately 4 μm. The homogeneity of the spectra was confirmed by analyzing several areas on a sample.

3. Results and discussion

3.1. $Bi_{1-x}Ca_xVO_{4-x/2}$ ($0 \le x \le 0.10$) pigments

Fig. 1 shows XRD patterns of the $Bi_{1-x}Ca_xVO_{4-x/2}$ ($0 \le x \le 0.10$) pigments. A single-phase monoclinic scheelite structure was observed for all pigments, and no diffraction peaks of impurities were evident in the patterns. The XRD peaks shifted to higher angles with increasing Ca^{2+} content, because Bi^{3+} (ionic radius: 0.117 nm) [40] in the host lattice is partially substituted by smaller Ca^{2+} (ionic radius: 0.112 nm) [40] ions. The monoclinic lattice volumes of the $Bi_{1-x}Ca_xVO_{4-x/2}$ pigments calculated from the diffraction angles in the XRD patterns are plotted in Fig. 2. The lattice volume of the monoclinic scheelite phase decreased monotonically with increasing Ca^{2+} concentration within the composition range of the single-phase scheelite structure ($0 \le x \le 0.10$), which indicates the formation of solid solutions.

Fig. 3 depicts UV–vis diffuse reflectance spectra for the $Bi_{1-x}Ca_xVO_{4-x/2}$ pigments. All samples exhibited strong optical absorption at wavelengths between 435 and 485 nm (*i.e.*, in the blue light region). The samples are yellow, because blue is the complementary color of yellow. The absorption intensity is significantly dependent on the calcium content. The $Bi_{0.92}Ca_{0.08}VO_{3.96}$ sample exhibited the highest absorption in the blue light region. The $L^*a^*b^*$ color coordinate data for the $Bi_{1-x}Ca_xVO_{4-x/2}$ pigments

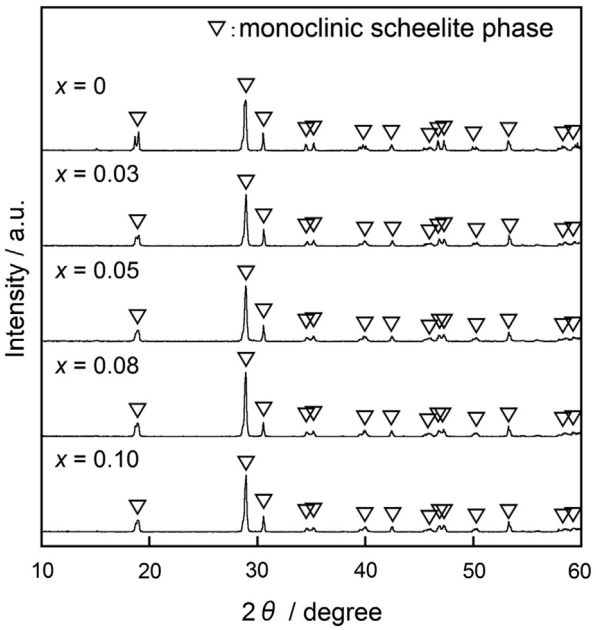

Fig. 1. XRD patterns of the $Bi_{1-x}Ca_xVO_{4-x/2}$ ($0 \le x \le 0.10$) pigments.

are summarized in Table 1. The L^*, a^*, and b^* values are dependent on the sample composition. $Bi_{0.92}Ca_{0.08}VO_{3.96}$ has the highest b^* value, which corresponds to the yellow component in the positive direction. Consequently, the $Bi_{0.92}Ca_{0.08}VO_{3.96}$ pigment has the most yellow hue of the $Bi_{1-x}Ca_xVO_{4-x/2}$ samples.

3.2. $Bi_{1-y}Zn_yVO_{4-y/2}$ ($0 \le y \le 0.10$) pigments

Fig. 4 shows XRD patterns of the $Bi_{1-y}Zn_yVO_{4-y/2}$ ($0 \le y \le 0.10$) pigments. As with the $Bi_{1-x}Ca_xVO_{4-x/2}$ pigments, a single-phase monoclinic scheelite structure was observed for all samples. In addition, the XRD peaks shifted to higher angles with increasing Zn^{2+} content, because the ionic radius of Zn^{2+} (0.090 nm) [40] is smaller than that of Bi^{3+} (0.117 nm) [40]. The monoclinic lattice volumes of the $Bi_{1-y}Zn_yVO_{4-y/2}$ pigments are also plotted in Fig. 2. The lattice volume of the monoclinic scheelite phase decreased monotonically with increasing Zn^{2+} content within the

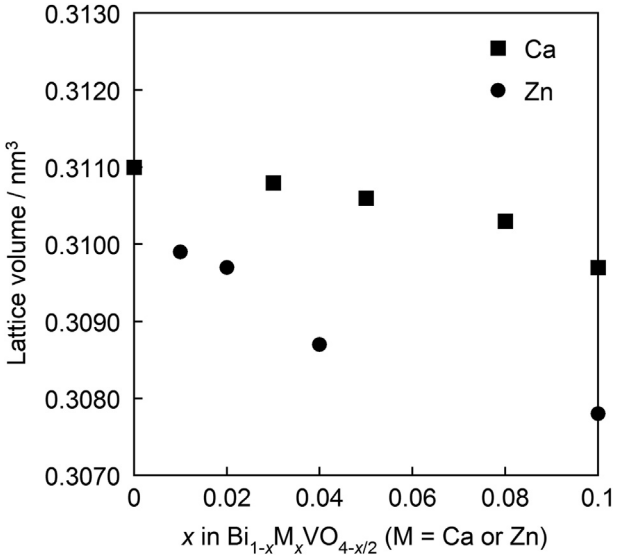

Fig. 2. Monoclinic lattice volumes of the $Bi_{1-x}M_xVO_{4-x/2}$ pigments (M = Ca or Zn).